

RFOT theory for glassy dynamics in a single condensed polymer

Hyun Woo Cho¹, Guang Shi¹, T. R. Kirkpatrick² and D. Thirumalai¹

¹*Department of Chemistry, University of Texas at Austin, Austin, Texas 78712, USA and*

²*Institute for Physical Science and Technology, University of Maryland, College Park, Maryland 20742, USA*

The number of compact structures of a single condensed polymer (SCP), with similar free energies, grows exponentially with the degree of polymerization. In analogy with structural glasses (SGs), we expect that at low temperatures chain relaxation should occur by activated transitions between the compact metastable states. By evolving the states of the SCP that is linearly coupled to a reference state, we show that, below a dynamical transition temperature (T_d), the SCP is trapped in a metastable state leading to slow dynamics. At a lower temperature, $T_K \neq 0$, the configurational entropy vanishes, resulting in a thermodynamic random first order ideal glass transition. The relaxation time obeys the Vogel-Fulcher-Tamman law, diverging at $T = T_0 \approx T_K$. These findings, accord well with the random first order transition theory, establishing that SCP and SG exhibit similar universal characteristics.

The discovery that a single chromosome (long mega base pair sized polymers) is heterogeneously organized [1] has triggered a keen interest in its dynamics. Experiments have suggested that glass-like behavior should be expected in chromosome dynamics [2], translocation of DNA [3, 4], collapse kinetics of polymers [5], and more recently intrinsically disordered proteins [6]. Dynamics [7–9], and phase behavior [10–12] of single (synthetic) polymers have also suggested that a single polymer displays glassy behavior upon cooling or compression, just like in bulk liquids that undergo a transition to glassy states [13–15]. However, it is unknown whether the glass transition in a single polymer, which is relevant in a number of unrelated systems, is governed by the same physical principles that describe their macroscopic counterparts.

Single condensed polymer (SCP) should exhibit glass like behavior because their phase space structure satisfies all the requirements for observing slow dynamics. At temperatures (T s) below the collapse temperature, T_θ , the number of compact structures or states, with similar free energies, scales exponentially with N [16]. The states are separated by large free energy barriers. At high temperatures, the relaxation dynamics is expected to be diffusive. At low temperatures, the exploration of the distinct compact structures can only occur by activated transitions. Thus, the physical picture for a SCP is exactly the same as in the structural glass transition (SGT). Therefore, we expect that the dynamics of the SCP should be described by theories developed for bulk glassy systems. In particular, we anticipate that the SCP dynamics, over a wide range of temperatures, can be understood within the framework of the Random First Order Transition (RFOT) theory. That this is so is the main conclusion of this work.

Let us describe the salient aspects of the energy landscapes of SCP and liquids that undergo the SGT. The dynamics in the latter case is well-described by the Random First Order Transition (RFOT) theory [17], developed based on precisely solvable models [18–20]. An im-

portant physical ingredient in the RFOT theory for the SGT is the emergence of an exponentially large number of metastable states with similar free energies [21] below a characteristic dynamic transition temperature T_d [18, 19]. At $T < T_d$, the system is trapped in a specific metastable state for a finite but long time period, and hence relaxation occurs only by activated transition. The free energy barrier, ΔF^\ddagger , between the metastable states is related to the configurational entropy, S_{conf} as $\Delta F^\ddagger \sim S_{\text{conf}}^{-1}$ [17]. Since S_{conf} decreases as T decreases, ΔF^\ddagger increases, resulting in a significant increase in the structural relaxation time. RFOT theory predicts that S_{conf} vanishes at an ideal glass transition temperature, $T_K < T_d$, at which a thermodynamic random first-order transition, without latent heat, from a super cooled liquid to an ideal glass occurs.

To affirm the predictions of the RFOT theory in the SCP, we use the Franz-Parisi (FP) method [22, 23], which involves coupling two copies of the system through a field with strength ϵ . FP showed that an order parameter measuring the structural similarity between the states exhibited first order transition at non-zero ϵ only when a large number of metastable states emerge. The FP method was developed further to establish the emergence of metastable states, and possible the existence of an ideal glass transition in model atomic glasses [24–28].

We used a standard bead-spring model for a polymer composed of a sequence of $N = 128$ Lennard-Jones (LJ) particles linearly connected by a harmonic potential (section I of the Supplementary Information (SI)). At low temperatures, the polymer is trapped in a metastable state instead of transitioning to an ordered state (section II in the SI). Following FP (Figure 1), we created two replicas (or samples) of the SCP at the same T . Replica 1 in Figure 1 represents a fixed reference conformation ($\{\vec{r}_0\}$), chosen from an equilibrium ensemble, and serves as a quenched random field. The conformation of $\{\vec{r}\}$ in replica Replica 2 (Figure 1) is evolved using Monte Carlo simulation by coupling it to Replica 1 through an external field (External field in Figure 1). The energy

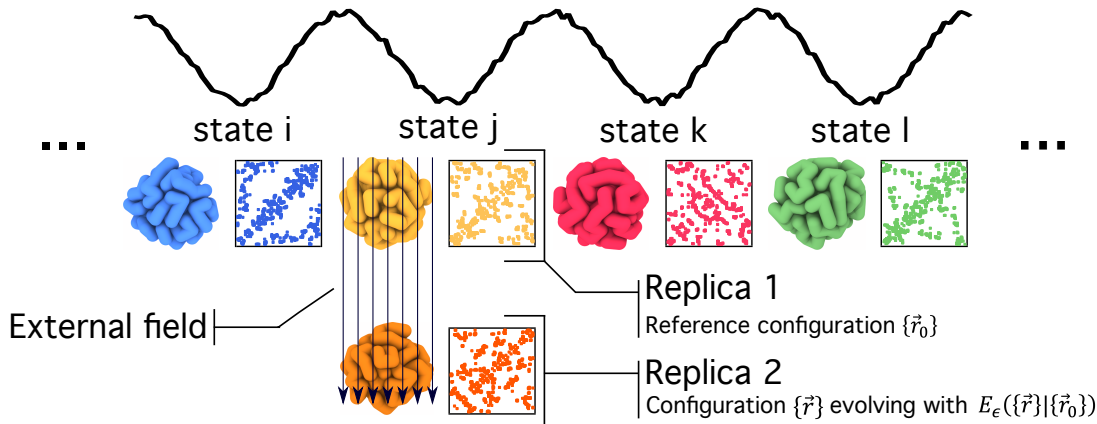


FIG. 1. **Numerical implementation of the Franz-Parisi (FP) method for polymers.** In the FP method, two replicas (Replica 1 and Replica 2) are coupled. The quenched reference conformation in Replica 1 is sampled from an ensemble of equilibrium SCP conformations. The conformation in Replica 1 represents one of the exponentially large number of metastable states. The conformation in Replica 2, coupled to Replica 1 by an external field, is evolved using the Monte Carlo method. The panels next to the snapshot represent the contact maps in the metastable states. The structural similarity between Replica 1 and Replica 2 is defined using the extent of overlap of the contact maps (blue and red for example).

$E_\epsilon(\{\vec{r}\}|\{\vec{r}_0\})$ of the coupled replicas is,

$$E_\epsilon(\{\vec{r}\}|\{\vec{r}_0\}) = E(\{\vec{r}\}) - N\epsilon Q_{\text{stat}}(\{\vec{r}\}, \{\vec{r}_0\}), \quad (1)$$

where $E(\{\vec{r}\})$ is the potential energy of the SCP in Replica 2, ϵ is the strength of the external field, and $Q_{\text{stat}}(\{\vec{r}\}, \{\vec{r}_0\})$ measures the structural similarity between $\{\vec{r}\}$ and $\{\vec{r}_0\}$.

By anticipating applications to chromosomes, we used contact maps, which can be inferred from cross-linking experiments [1], to calculate Q_{stat} . The contact map is a low dimensional representation of given structure of the SCP, as are the Hi-C maps for the chromosomes. Two monomers that are not covalently linked to each other are in contact if the distance between them is less than $R_c = 1.4\sigma$, corresponding to the first minimum in the radial distribution function (section II in the SI). Panels next to the snapshots in Figure 1 illustrate examples of the contact maps, where the pairs of non-bonded monomers in contact are projected onto a two dimensional space.

The static overlap function Q_{stat} is calculated using,

$$Q_{\text{stat}}(\{\vec{r}\}, \{\vec{r}_0\}) = \frac{\sum_{(i,j)'} q_{ij}(\{\vec{r}\}) q_{ij}(\{\vec{r}_0\})}{\sum_{(i,j)'} q_{ij}(\{\vec{r}_0\})}, \quad (2)$$

where $q_{ij}(\{\vec{r}\})$ is the contact function of configuration $\{\vec{r}\}$, which is unity if i and j monomers are in contact and zero otherwise, and $(i, j)'$ indicates that the sum is over all non-bonded pairs of monomers. If $\{\vec{r}\}$ and $\{\vec{r}_0\}$ are identical, $Q_{\text{stat}}(\{\vec{r}\}, \{\vec{r}_0\})=1$. On the other hand, if the replicas are totally uncorrelated, Q_{stat} is the average contact probability $\langle q_{ij} \rangle$, which is found to be $\simeq 0.13$ for the parameters used in the simulations. From Eqs (1) and (2), it follows that Q_{stat} varies as a function of ϵ .

When the external field strength, ϵ , is sufficiently large, $\{\vec{r}\}$ is highly biased to $\{\vec{r}_0\}$, such that $Q_{\text{stat}} \simeq 1$. If ϵ decreases to 0, $\{\vec{r}\}$ is independent of $\{\vec{r}_0\}$, resulting in $Q_{\text{stat}} \simeq \langle q_{ij} \rangle$.

It is important to note that the expected changes in Q_{stat} with $\epsilon \neq 0$ should have the characteristics of first order transition only if metastable states are probed. The randomly-chosen equilibrium configurations in Replica 1 is an example of a particular metastable state (Figure 1). Since all the metastable states are generated at the same thermodynamic condition (the same T and N), they are equivalent. The individual free energy is F_α where α is a label for the metastable state. The canonical free energy F_{tot} is less than the component averaged free energy, $\sum_\alpha P_\alpha F_\alpha$, where P_α is the probability of being in the state α [17, 29, 30]. The difference between the two is TS_{conf} , which is the entropic gain arising from an exploration of all possible states, $F_{\text{tot}} = F_\alpha - TS_{\text{conf}}$. Thus, if ϵ is strong enough to compensate for the entropic penalty, the SCP in Replica 2 would be trapped in a single metastable state of the SCP, such that $Q_{\text{stat}} = Q_{\text{glass}} \simeq 1$. Otherwise, it could explore all possible metastable states over time, resulting in Q_{stat} being equal to $Q_{\text{liquid}} = \langle q_{ij} \rangle$. This argument shows that, at the critical value of $\epsilon = \epsilon_c$ where $N\epsilon_c(Q_{\text{glass}} - Q_{\text{liquid}}) \simeq TS_{\text{conf}}$, Q_{stat} should change discontinuously between Q_{glass} and Q_{liquid} , which would be a signature of a first order transition. Thus, by showing Q_{stat} exhibits the first-order-like transition at $\epsilon \neq 0$, we can confirm the existence of metastable states in the SCP.

In the upper panel of Figure 2 (A), $\langle Q_{\text{stat}} \rangle$ is plot-

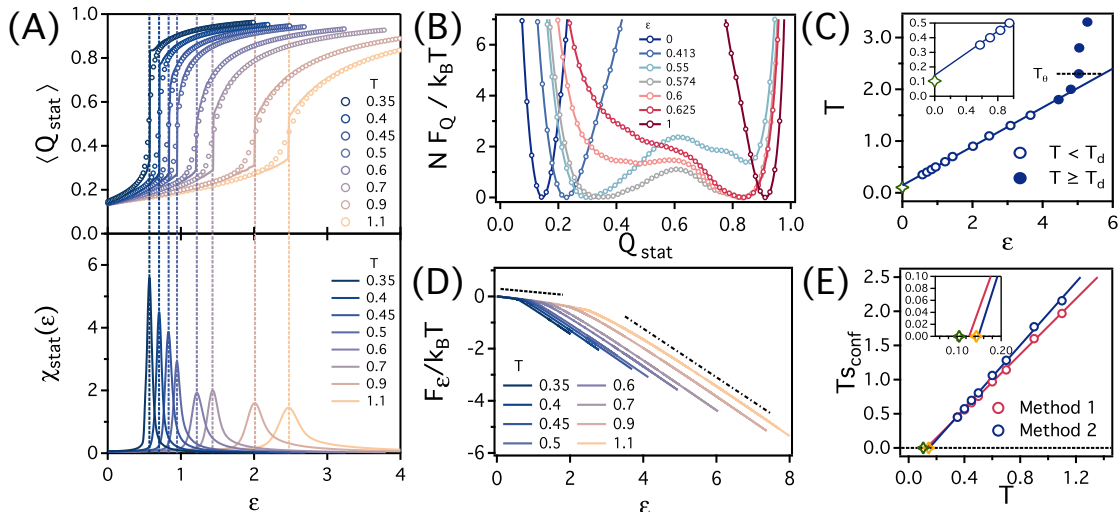


FIG. 2. **Phase behavior of Q_{stat} .** (A) Average $\langle Q_{\text{stat}} \rangle$ (the upper panel) and susceptibility $\chi_{\text{stat}}(\epsilon)$ (the lower panel) of the order parameters with respect to ϵ for various T . The vertical dashed lines represent the position of ϵ where $\chi_{\text{stat}}(\epsilon)$ has the maximum value. The solid lines represent the position of Q_{stat} where F_Q in (B) has the minimum value. (B) F_Q of various ϵ at $T=0.35$. F_Q in the graph is shifted by its minimum value. (C) $T - \epsilon$ phase diagram of Q_{stat} . The open and filled symbols represent T of ϵ_c for $T < T_d$ and $T \geq T_d$, respectively. The solid line is a linear fit for $T < T_d$. The black dashed line denotes the position of T_θ . The open green star denotes T_0 . The inset is the same phase diagram at $0 \leq \epsilon \leq 0.9$. (D) F_ϵ as a function of ϵ for various T . F_ϵ is shifted by $F_{\epsilon=0}$. The slopes of the dashed and dashed-dotted lines are -0.13 and -0.93 , respectively. (E) T_{sconf} of single polymers as a function of T . The solid lines are their linear fits. The yellow and green open symbols represent T_0 and y intercept of the solid line in (C), respectively. In the inset, we magnify the graph near the x intercepts of the linear fits.

ted as a function of ϵ for various T (the open symbols), where $\langle \dots \rangle$ is a double average over thermal and disorder fluctuation; we first perform an average of Q_{stat} over thermal fluctuations with $\{\bar{r}_0\}$ fixed, and then an average over various $\{\bar{r}_0\}$ is calculated to account for disorder fluctuations (details are in section II of the SI). As expected, $\langle Q_{\text{stat}} \rangle$ decreases from $\simeq 1$ to $\langle q_{ij} \rangle \simeq 0.13$ as ϵ decreases to 0. The static susceptibility, $\chi_{\text{stat}}(\epsilon) = N(\langle Q_{\text{stat}}^2 \rangle - \langle Q_{\text{stat}} \rangle^2)$, has a peak at the value of ϵ where $\langle Q_{\text{stat}} \rangle$ drastically changes (the dashed vertical lines in Figure 2 (A)). The width of the peaks decreases dramatically and the amplitudes increase as T decreases, reflecting a sharp change in $\langle Q_{\text{stat}} \rangle$ at low values of T . Such dramatic changes in $\langle Q_{\text{stat}} \rangle$ and $\chi_{\text{stat}}(\epsilon)$ are particularly striking considering the relatively small size of the polymer, and provides evidence for the first-order like phase transition in the presence of the coupling field.

Next, we confirm that the abrupt change in Q_{stat} indeed reflects a regular first order transition. In the first order transition, the minimum in the free energy F_Q as a function of Q_{stat} changes discontinuously at the phase transition point. The free energy, F_Q , is calculated from the distribution $P(Q_{\text{stat}})$ as, $-\frac{NF_Q}{k_B T} = \langle \ln P(Q_{\text{stat}}) \rangle$. In Figure 2 (B), F_Q at $T = 0.35$ is plotted as a function of Q_{stat} for various ϵ . When $\epsilon = 1$, F_Q has minimum at $Q_{\text{stat}} \simeq 0.93$, indicating that $\{\bar{r}\}$ stays around the metastable state associated with $\{\bar{r}_0\}$. As ϵ decreases to

0, the minimum shifts to $Q_{\text{stat}} = 0.13$. At $\epsilon = 0.574$, where χ_{stat} has a maximum, F_Q has two minima at $Q_{\text{stat}} \approx 0.34$ and $Q_{\text{stat}} \approx 0.84$. This means that the two different states coexist at $\epsilon = 0.574$, which leads to a discontinuous change in the order parameter. In Figure 2 (A), we plot the minimum position of F_Q as a function of ϵ for various T (the solid lines). As shown in the graph, the minimum position changes discontinuously at ϵ where the fluctuation of Q_{stat} is maximized, revealing the first order nature of the transition.

We arrive the same conclusion from the Ehrenfest classification of the phase transition. According to Ehrenfest classification, the first derivative of the free energy F_ϵ with respect to ϵ should be discontinuous at the transition point. We obtained F_ϵ from F_Q by the Legendre transformation,

$$F_\epsilon = F_Q - \epsilon Q_{\text{stat}}, \quad (3)$$

where ϵ is equal to $\epsilon = \partial F_Q / \partial Q_{\text{stat}}$ [31]. Figure 2 (D), which displays F_ϵ as a function of ϵ for various T , shows a discontinuous change in the slopes ($= dF_\epsilon / d\epsilon$) between -0.13 and -0.93 (the dashed and dashed-dotted lines, respectively), which is a signature of the first order transition. Since $Q_{\text{stat}} = -\frac{dF_\epsilon}{d\epsilon}$ (Eq (3)), we define the effective order parameters in the two states as $Q_{\text{liquid}} = 0.13$ and $Q_{\text{glass}} = 0.93$. Thus, the discontinuous change in the slope in figure 2 (D) corresponds to the discontinuous

change in Q_{stat} between Q_{liquid} and Q_{glass} . Figures 2 (B) and (D) confirm that the first order transition in Q_{stat} occurs with a change in ϵ , thus verifying the existence of the metastable states in the SCP with $N = 128$. We also find that the first order transition as N increases, indicating that the metastable states should exist more stably in the SCP as $N \rightarrow \infty$ (section III in the SI).

RFOT theory predicts that metastable states, separated by barriers, should cease to exist above the dynamical transition temperature T_d , which implies that the first-order transition nature of Q_{stat} should disappear at $T > T_d$. We found that Q_{stat} changes continuously with ϵ when $T \geq 1.8$ (see section III of the SI), indicating the disappearance of the metastable states at $T > T_d \simeq 1.8$. The collapse temperature is determined to be $T_\theta = 2.3 > T_d$ (section II in the SI). Thus, the equilibrium collapse transition occurs before the dynamical transition, implying that the dynamics of the SCP in the temperature $T_d \leq T \leq T_\theta$ can be described by the standard polymer theory. Only below T_d the dynamics is determined by activated transitions between equivalent compact structures.

The phase behavior in Figure 2 (A) is summarized in Figure 2 (C). The phase boundaries (ϵ_c, T_c) are associated with the peak positions in χ_{stat} at a given T (the open symbols in the graph). At $T < T_d$ (the open symbols), Q_{stat} changes discontinuously, and when $T > T_d$ (the filled triangles), Q_{stat} changes continuously. Above T_θ (the black dashed lines), ϵ_c is less dependent on T . Because T_c changes linearly with ϵ_c (when $T < T_d$), we extrapolate the phase boundary to $\epsilon = 0$ (the blue solid line). The y intercept in the linear fit indicates T_c at $\epsilon = 0$. In the SCP, T_c has a positive value at $\epsilon = 0$ ($T_c(\epsilon = 0) = 0.14$), which signals that a thermodynamic transition (see below for the nature of the transition) would occur at the non-zero temperature when $\epsilon = 0$. This means that the free energy of individual metastable states F_α is equal to the total free energy F_{tot} at a finite temperature even without external fields, which is only possible if $S_{\text{conf}} = 0$ at $T_c(\epsilon = 0)$.

We, therefore, investigated if S_{conf} does indeed vanish at $T_c(\epsilon = 0)$. Using two methods introduced elsewhere [27, 32], S_{conf} at $\epsilon = 0$ is estimated as a function of T . Since the first order transition occurs when the entropic gain (TS_{conf}) is compensated by the energetic contribution of the fields ($N\epsilon_c(Q_{\text{glass}} - Q_{\text{liquid}})$), we estimated the configurational entropy per monomer $s_{\text{conf}} = S_{\text{conf}}/N$ using (Method 1) [27], $TS_{\text{conf}} = \epsilon_c[Q_{\text{glass}} - Q_{\text{liquid}}]$. A more natural way is to calculate TS_{conf} as the difference between F_α and F_{tot} , which corresponds to $F_{Q_{\text{glass}}}$ and $F_{Q_{\text{liquid}}}$ at $\epsilon = 0$, respectively. Thus, S_{conf} can also be calculated using,

$$TS_{\text{conf}} = F_{Q_{\text{glass}}}(\epsilon = 0) - F_{Q_{\text{liquid}}}(\epsilon = 0). \quad (4)$$

Figure 2 (E) plots TS_{conf} (the open symbols) as a function of T using Method 1 and (Eq. 4). Linear extrapolation

of TS_{conf} (the linear lines) shows that s_{conf} vanishes at a similar non-zero value of T , regardless of which method is employed. It should be emphasized that the numerical value of the temperature is consistent with $T_c(\epsilon = 0)$ (the open yellow star). This confirms that it is because the configurational entropy vanishes that the thermodynamic transition occurs at $T_c(\epsilon = 0)$.

What is the nature of the thermodynamic transition of the SCP at $T_c(\epsilon = 0)$? First, this corresponds to an ideal glass transition of the SCP. Most importantly, we note from Eq (4), TS_{conf} is the energy difference between the two states, which accounts for the latent heat at the transition. Therefore, Figure 2 (E) shows that as T approaches $T_c(\epsilon = 0)$, the latent heat decreases and vanishes at $T_c(\epsilon = 0)$. This implies that at $T_c(\epsilon = 0)$, the SCP exhibits a *random* first order transition from liquid to an ideal glass without releasing latent heat but with a discontinuity in Q_{stat} . This is the fundamental feature of the ideal glass transition anticipated in the RFOT theory. Hence, Figures 2 (C) and (E) show that the ideal glass transition in the SCP at $T_K = T_c(\epsilon = 0) \neq 0$ is truly the analogue of T_K in bulk glasses.

Another major prediction made in our earlier studies is that there is a consistency between thermodynamic random first order transition and the underlying dynamics [33]. To investigate the dynamics of the SCP, we performed dynamic MC simulations (details in the SI). We define the time dependent overlap function $Q_{\text{dyn}}(t)$ as,

$$Q_{\text{dyn}}(t) = \frac{\sum_{(i,j)} q_{ij}(t)q_{ij}(0)}{\sum_{(i,j)} q_{ij}(0)}, \quad (5)$$

where $q_{ij}(t)$ is the contact function of a single polymer at time t ; $Q_{\text{dyn}}(t)$ quantifies how rapidly the contact map loses memory of the initial pattern. By definition $Q_{\text{dyn}}(t = 0) = 1$. As $t \rightarrow \infty$, the SCP loses memory of the structural correlation, and thus the pattern of the contact map also becomes independent of the initial state. Consequently, $Q_{\text{dyn}}(t)$ decays to $\langle q_{ij} \rangle$.

Figure 3 (A) shows $Q_{\text{dyn}}(t)$ as a function of t at different T . As T decreases from 1.1 to 0.35, $Q_{\text{dyn}}(t)$ decays more slowly with the decay time constant increasing by a few orders of magnitude. Figure 3 (B) shows that heights and timescales of the peak in the dynamic susceptibility, χ_{dyn} , $\chi_{\text{dyn}}(t) = N[\langle Q_{\text{dyn}}(t)^2 \rangle - \langle Q_{\text{dyn}}(t) \rangle^2]$ increase as T decreases, implying that the structural relaxation becomes heterogeneous as T decreases [34–36]. Thus, Figures 3 (A) and (B) reveal that the sluggish structural relaxation in the SCP is accompanied by enhanced dynamic heterogeneity, which is an important dynamic property of glassy liquids [37–39].

We estimated the structural relaxation time τ_α using $Q_{\text{dyn}}(t = \tau_\alpha) = 0.3$. Figure 3 (C) shows that τ_α increases by more than two orders of magnitude when T decreases from 1.1 to 0.35 (the open symbols). Such a large increase in τ_α in a finite sized polymer is substantial. The

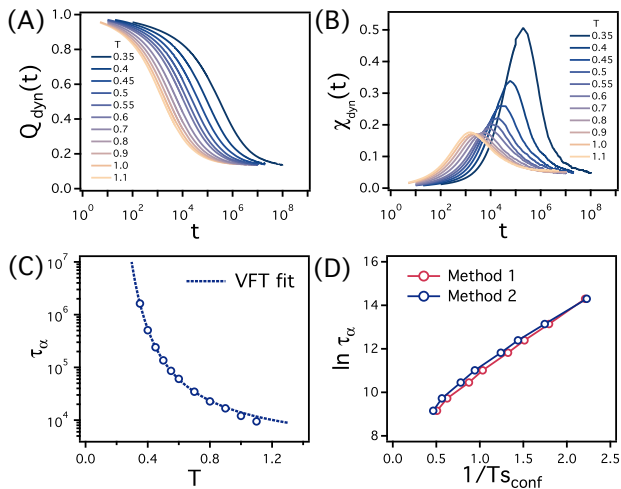


FIG. 3. **Glassy dynamics in the SCP.** (A) Time dependent overlap function $Q_{\text{dyn}}(t)$ and (B) susceptibility $\chi_{\text{dyn}}(t)$ for various T . (C) Dependence of τ_α on T (the open symbols). The dashed line is the VFT fit. (D) Relation between τ_α and s_{conf} .

sharp increase in τ_α in the SCP as well as in metallic [40], colloidal systems [41], and molecular glasses [42], is described well by the Vogel-Tamman-Flucher (VFT) equation, $\tau_\alpha = \tau_0 \exp[\frac{D_0 T_0}{T - T_0}]$, where τ_0 , D_0 and T_0 are fitting parameters. We fit the calculated τ_α as a function of T to the VFT equation (the dashed line in Figure 3 (C)), which gives $T_0 = 0.1$, (the green open symbols in Figure 2 (C) and (E) the temperature at which τ_α diverges. The value of T_0 is close to T_K .

The divergence of τ_α is closely associated with the decrease in s_{conf} . A scaling relation exists between τ_α and s_{conf} of bulk liquids, $\ln \tau_\alpha \sim 1/Ts_{\text{conf}}$ [17]. In Figure 3 (D), we plot $\ln \tau_\alpha$ as a function of Ts_{conf} obtained using Method 1 and (4). There is a modest deviation from a linear line possibly due to the confined geometry of the SCP. Nevertheless, this graph clearly shows that the increase in τ_α is closely related to the decrease in s_{conf} , implying a causal relationship between the two quantities in the finite-sized SCP. Thus, the dynamics and statics of the SCP are consistently predicted by the RFOT theory.

The glassy behavior illustrated in Figures 2 and 3 for the SCP is shared by bulk liquid glasses. Amorphous metastable states in bulk liquid glasses was also probed by the FP method [24–27]. And, the same relation between configurational entropy and relaxation time was found. The fluctuations of order parameters associated with the SCP appears to belong to the random field Ising model (RFIM) universality class (section IV in the SI) in the presence of the quenched field.

Our findings show that the essence of the RFOT theory holds for a diverse systems that undergo liquid to glass transition. It appears that the difficulty in accessing the ideal glass transition temperature in atomic glasses is

greatly lessened in the SCP. The use of the coupling field allows us to probe the energy landscape readily. We will be remiss if we do not stress that the random first order transition at T_K , with $\epsilon = 0$ that we establish by suitable numerical methods within the FP scheme, differs from the line of first order transitions that occur at $\epsilon_c \neq 0$. In the SCP, the transition is from a disordered state to an ordered compact state. The dynamics in the disordered state can be described using well-known theory above T_d whereas below T_d polymer dynamics requires RFOT theory for capturing the activated transition. Finally, the SCP, and more importantly the much larger chromosomes that are compact and exhibit glass-like dynamics [43], could be ideal systems to explore RFOT concepts.

Acknowledgements: This work was supported by NSF (CHE 19-00093), and the Welch Foundation Grant F-0019 through the Collie-Welch chair.

- [1] E. H. Finn and T. Misteli, *Science* **365** (2019).
- [2] I. Bronshtein, E. Kepten, I. Kanter, S. Berezin, M. Lindner, A. B. Redwood, S. Mai, S. Gonzalo, R. Foisner, Y. Shav-Tal, et al., *Nat. Comm.* **6** (2015).
- [3] Z. T. Berendsen, N. Keller, S. Grimes, P. J. Jardine, and D. E. Smith, *Proc. Natl. Acad. Sci. USA* **111**, 8345 (2014).
- [4] N. Keller, S. Grimes, P. J. Jardine, and D. E. Smith, *Nat. Phys.* **12**, 757 (2016).
- [5] S. Kwon, H. W. Cho, J. Kim, and B. J. Sung, *Phys. Rev. Lett.* **119**, 087801 (2017).
- [6] I. L. Morgan, R. Avinery, G. Rahamim, R. Beck, and O. A. Saleh, *Phys. Rev. Lett.* **125**, 058001 (2020).
- [7] T. T. Perkins, S. R. Quake, D. E. Smith, and S. Chu, *Science* **264**, 822 (1994).
- [8] F. Latinwo and C. M. Schroeder, *Soft Matter* **7**, 7907 (2011).
- [9] M. V. Tamm, L. I. Nazarov, A. A. Gavrilov, and A. V. Chertovich, *Phys. Rev. Lett.* **114**, 178102 (2015).
- [10] K. Yoshikawa, M. Takahashi, V. V. Vasilevskaya, and A. R. Khokhlov, *Phys. Rev. Lett.* **76**, 3029 (1996).
- [11] F. Rampf, K. Binder, and W. Paul, *J. Polym. Sci. B Polym. Phys.* **44**, 2542 (2006).
- [12] M. P. Taylor, W. Paul, and K. Binder, *J. Chem. Phys.* **131**, 114907 (2009).
- [13] N. V. Dokholyan, E. Pitard, S. V. Buldyrev, and H. E. Stanley, *Phys. Rev. E* **65**, 030801 (2002).
- [14] M. Tress, E. U. Mapesa, W. Kossack, W. K. Kipnusu, M. Reiche, and F. Kremer, *Science* **341**, 1371 (2013).
- [15] W. L. Merling, J. B. Mileski, J. F. Douglas, and D. S. Simmons, *Macromolecules* **49**, 7597 (2016).
- [16] H. Orland, C. Itzykson, and C. Dedominicis, *J. de Physique Lett.* **46**, L353 (1985).
- [17] T. R. Kirkpatrick, D. Thirumalai, and P. G. Wolynes, *Phys. Rev. A* **40**, 1045 (1989).
- [18] T. R. Kirkpatrick and D. Thirumalai, *Phys. Rev. Lett.* **58**, 2091 (1987).
- [19] T. R. Kirkpatrick and D. Thirumalai, *Phys. Rev. B* **36**, 5388 (1987).
- [20] T. R. Kirkpatrick and P. G. Wolynes, *Phys. Rev. B* **36**,

- 8552 (1987).
- [21] M. Goldstein, *J. Chem. Phys.* **51**, 3728 (1969).
- [22] S. Franz and G. Parisi, *Phys. Rev. Lett.* **79**, 2486 (1997).
- [23] S. Franz and G. Parisi, *J. Stat. Mech.* **2013**, P11012 (2013).
- [24] L. Berthier, *Phys. Rev. E* **88**, 022313 (2013).
- [25] G. Parisi and B. Seoane, *Phys. Rev. E* **89**, 022309 (2014).
- [26] L. Berthier and R. L. Jack, *Phys. Rev. Lett.* **114**, 205701 (2015).
- [27] L. Berthier and D. Coslovich, *Proc. Natl. Acad. Sci. USA* **111**, 11668 (2014).
- [28] L. Berthier, P. Charbonneau, D. Coslovich, A. Ninarello, M. Ozawa, and S. Yaida, *Proc. Natl. Acad. Sci. USA* **114**, 11356 (2017).
- [29] R. Palmer, *Adv. Phys.* **31**, 669 (1982).
- [30] T. R. Kirkpatrick and D. Thirumalai, *Rev. Mod. Phys.* **87**, 183 (2015).
- [31] M. Mézard and G. Parisi, *Glasses and Replicas* (John Wiley & Sons, Ltd, 2012), chap. 4, pp. 151–191, ISBN 9781118202470.
- [32] L. Berthier, M. Ozawa, and C. Scalliet, *J. Chem. Phys.* **150**, 160902 (2019).
- [33] T. R. Kirkpatrick and D. Thirumalai, *J. Phys. A* **22**, L149 (1989).
- [34] T. R. Kirkpatrick and D. Thirumalai, *Phys. Rev. A* **37**, 4439 (1988).
- [35] E. Flenner, M. Zhang, and G. Szamel, *Phys. Rev. E* **83**, 051501 (2011).
- [36] E. Flenner and G. Szamel, *Phys. Rev. Lett.* **105**, 217801 (2010).
- [37] M. D. Ediger, C. A. Angell, and S. R. Nagel, *J. Phys. Chem.* **100**, 13200 (1996).
- [38] M. D. Ediger, *Ann. Rev. Phys. Chem.* **51**, 99 (2000).
- [39] G. Biroli and J. P. Garrahan, *J. Chem. Phys.* **138**, 12A301 (2013).
- [40] R. Busch, W. Liu, and W. L. Johnson, *J. Appl. Phys.* **83**, 4134 (1998).
- [41] H. W. Cho, M. L. Mugnai, T. R. Kirkpatrick, and D. Thirumalai, *Phys. Rev. E* **101**, 032605 (2020).
- [42] C. A. Angell, *Science* **267**, 1924 (1995).
- [43] H. Kang, Y.-G. Yoon, D. Thirumalai, and C. Hyeon, *Phys. Rev. Lett.* **115**, 198102 (2015).

Supplementary Information for

“RFOT theory for glassy dynamics in a single condensed polymer”

Hyun Woo Cho¹, Guang Shi¹, T. R. Kirkpatrick² and D. Thirumalai¹

¹*Department of Chemistry, University of Texas at Austin, Austin, Texas 78712, USA and*

²*Institute for Physical Science and Technology, University of Maryland, College Park, Maryland 20742, USA*

(Dated: September 14, 2020)

I. SIMULATION MODEL AND METHODS

1. Single polymer model

We consider a single polymer consisting of $N = 128$ beads that are linearly connected by a harmonic potential, $E_{\text{bond}}(r) = \frac{1}{2}k_b(r - r_0)^2$ where r is the distance between two bonded monomers, and the parameters k_b and r_0 are taken to be $2,000\epsilon_{LJ}/\sigma^2$ and $0.9/\sigma$, respectively. Pairs of monomers i and j that are separated along the polymer by more than two bonds with a spatial distance, r_{ij} , interact via a Lennard-Jones (LJ) potential, $E_{\text{pair}}(r_{ij}) = 4\epsilon_{LJ}[(\sigma/r_{ij})^{12} - (\sigma/r_{ij})^6]$. We truncate and shift the LJ potential, setting it to zero at $r_{ij} = 2.5\sigma$. In the simulations, ϵ_{LJ} and σ are the units of energy and length, respectively.

2. Preparation of equilibrium conformations

We performed parallel tempering Monte Carlo (PTMC) simulations [1] to efficiently sample the equilibrium configurations of the polymers. We used $n_r = 32$ independent replicas containing a single polymer at temperatures T_i with $T_1 < T_2 < \dots < T_{n_r-1} < T_{n_r=32}$. In the PTMC simulations, the positions of the polymers in the replicas are evolved independently. A monomer is randomly chosen and displaced by $\vec{\delta}$ whose components are uniformly sampled from $[-0.05, 0.05]$. The trial position is accepted using the standard Metropolis acceptance probability, $p = \min[1, \exp[-(E_n - E_o)/k_B T]]$, where E_n and E_o are the potential energies of the trial and original configurations, respectively, and the Boltzmann constant k_B is set to unity. We define Monte Carlo steps (MCSs) as the total number of attempted translational moves divided by n_r , the number of replicas. At every $N_{\text{swap}} = 10^4$ MCSs, two neighboring replicas i and $i + 1$ are randomly selected, and their configurations are swapped with a probability $p = \min[1, \exp[(1/k_B T_i - 1/k_B T_{i+1})(E_i - E_{i+1})]]$, where E_i is the potential energy of the i^{th} replica.

We carried out three sets of the PTMC simulations. In the first set, T ranges from $T_1 = 0.35$ to $T_{32} = 1.125$ with $T_{\text{gap}} = 0.025$, where T_{gap} is a temperature difference between the neighboring replicas, $T_{\text{gap}} = T_{i+1} - T_i$. $(T_1, T_{32}; T_{\text{gap}})$ in the second and third sets are $(1.2, 2.75; 0.05)$ and $(2.8, 4.35; 0.05)$, respectively. All sets of the simulations are run for 10^8 MCSs.

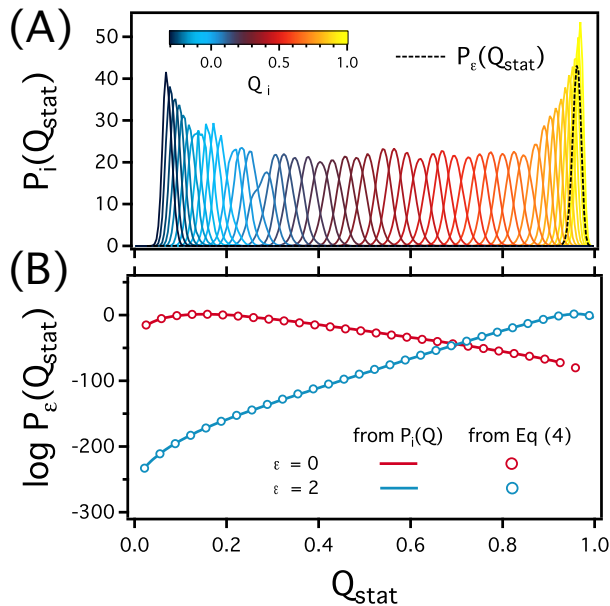


FIG. 1. (A) Distributions of Q_{stat} , $P_i(Q_{\text{stat}})$, calculated using $n_r = 48$ replicas at $T = 0.35$ and $\epsilon = 2$. The curves are colored according to the value of Q_i . $P_\epsilon(Q_{\text{stat}})$ is obtained from unbiased $P_i(Q_{\text{stat}})$ using Eqs (2) and (3) (the black dashed curve). (B) The distributions of Q_{stat} at $T = 0.35$ with $\epsilon = 0$ is in red, and $\epsilon = 2$ is given by the blue curve. Two independent HREMC (Hamiltonian replica exchange MC) simulations were carried out for $\epsilon = 0$ and 2, then $P_\epsilon(Q_{\text{stat}})$ (the solid curves) were obtained by reconstructing $P_i(Q_{\text{stat}})$ as in (A). The open symbols represent $P_\epsilon(Q_{\text{stat}})$ obtained from one another using Eq (4). The two methods result in identical $P_\epsilon(Q_{\text{stat}})$.

3. Estimation of $\langle Q_{\text{stat}} \rangle$ and χ_{stat}

We calculated $\langle Q_{\text{stat}} \rangle$ and χ_{stat} from the distribution $P_\epsilon(Q_{\text{stat}})$ using $\langle Q_{\text{stat}} \rangle = \int_0^1 Q P_\epsilon(Q) dQ$ and $\chi_{\text{stat}} = N(\langle Q_{\text{stat}}^2 \rangle - \langle Q_{\text{stat}} \rangle^2)$, where $\langle Q_{\text{stat}}^2 \rangle = \int_0^1 Q^2 P_\epsilon(Q) dQ$. In order to obtain $P_\epsilon(Q_{\text{stat}})$, over a broad range of Q_{stat} , we used umbrella sampling technique while implementing the Hamiltonian replica exchange MC (HREMC) simulations [2–4]. We used $n_r = 48$ replicas, and the energy function E_i of each replica is expressed as,

$$E_i = E_\epsilon(\{\vec{r}\}|\{\vec{r}_0\}) + E_{Q_i}(Q_{\text{stat}}), \quad (1)$$

where i is the index of the replicas, and $E_{Q_i}(Q_{\text{stat}})$ is a harmonic bias potential expressed as $E_{Q_i}(Q_{\text{stat}}) = NW(Q_i - Q_{\text{stat}})^2$, which restricts the distribution of Q_{stat} , $P_i(Q_{\text{stat}})$, near Q_i . The position of the single polymer in each replica is evolved via MC simulations for N_{swap} MCSs in the same way as in the PTMC simulations. At every N_{swap} , the configurations of neighboring replicas are swapped with a probability $p = \min[1, \exp[(E_i - E_{i+1})/k_B T]]$. The strength of the bias potential, W , in this simulation is $4\epsilon_{LJ}$ and Q_i 's of each replica are taken for their distributions to cover

a full range of Q_{stat} from 0 to 1 as shown in Figure 1 (A). N_{swap} ranges from 10^3 to 10^4 MCSs and the simulations are run for 5×10^6 to 10^8 MCSs. Note that $P_\epsilon(Q_{\text{stat}})$ is expressed in terms of P_i 's [1],

$$P_\epsilon(Q_{\text{stat}}) = \frac{\sum_{i=1}^{n_r} P_i(Q_{\text{stat}})}{\sum_{i=1}^{n_r} g_i \exp[-E_{\text{bias}}(Q_i)/k_B T]}, \quad (2)$$

where g_i obeys,

$$g_i^{-1} = \int_0^1 dQ \frac{\sum_{j=1}^{n_r} P_j(Q)}{\sum_{j=1}^{n_r} g_j \exp[[E_{Q_i}(Q) - E_{Q_j}(Q)]/k_B T]}. \quad (3)$$

The values of g_i were obtained in a self-consistent manner using Eq (3), from which $P_\epsilon(Q_{\text{stat}})$ was determined by Eq (2) (the dashed line in Figure 1 (A)).

Note that for a given set of $\{\vec{r}_0\}$ and T , the distributions of Q_{stat} with two different ϵ values, say ϵ_1 and ϵ_2 , follow a relation,

$$P_{\epsilon_1}(Q_{\text{stat}}) = \frac{P_{\epsilon_2}(Q_{\text{stat}}) \exp[-Q_{\text{stat}} \Delta \epsilon / k_B T]}{\int_0^1 dQ P_{\epsilon_2}(Q) \exp[-Q \Delta \epsilon / k_B T]}, \quad (4)$$

where $\Delta \epsilon$ is $\epsilon_1 - \epsilon_2$. Figure 2 confirms the validity of Eq (4). First, we evaluate $P_\epsilon(Q_{\text{stat}})$ at $\epsilon = 0$ and 2 with same $\{\vec{r}_0\}$ with $T = 0.35$ through Eqs (1) to (3) (the solid lines in Figure 2). Then, we obtain one from the other using Eq (4) (the open circles). As shown in the graph, both the methods result in identical $P_\epsilon(Q_{\text{stat}})$. This suggests that $P_\epsilon(Q_{\text{stat}})$, over broad ranges of ϵ , can be calculated from a single $P_\epsilon(Q_{\text{stat}})$ without carrying out multiple HREMC simulations. Hence, we (1) chose $\{\vec{r}_0\}$ at T among the equilibrium configurations obtained by the PTMC simulation, (2) estimated $P_{\epsilon=0}(Q_{\text{stat}})$ with the HREMC simulations, and (3) determine $P_\epsilon(Q_{\text{stat}})$ at various ϵ from $P_{\epsilon=0}(Q_{\text{stat}})$ using Eq (4). The distributions at each ϵ are averaged over 80 to 112 values of $\{\vec{r}_0\}$.

4. Dynamic Monte Carlo simulation

In order to investigate the dynamics of a single condensed polymer (SCP), we carried out dynamic Monte Carlo (dMC) simulations, where at every MCS, a randomly chosen monomer was displaced by $\vec{\delta}$ and the resulting configuration was accepted using the standard Metropolis criterion, as in the PTMC simulation. The maximum displacement of each component of $\vec{\delta}$ is 0.01σ . The MCS (the number of attempted translational moves) normalized by N is used as the unit of time.

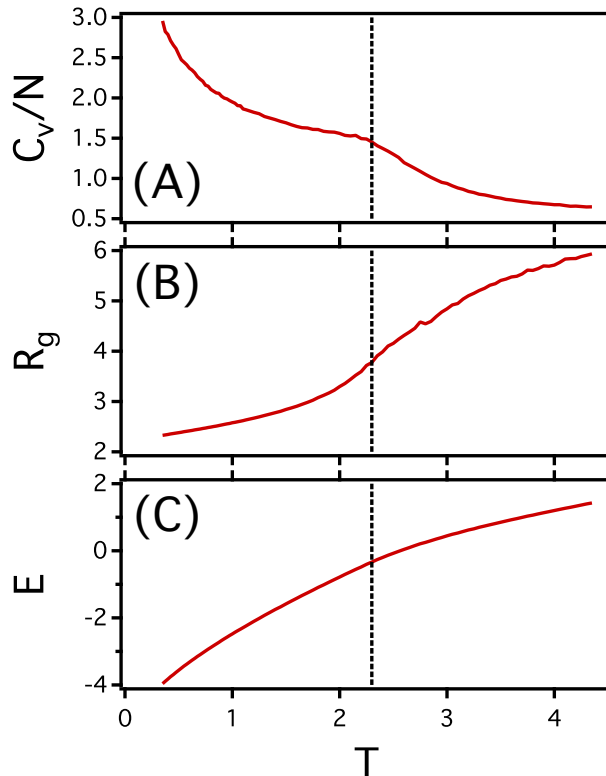


FIG. 2. (A) C_v , (B) R_g , and (C) E of the single polymer as a function of T . The black dashed line indicates the transition temperature T_θ where C_v has a shoulder-like structure.

II. CONFORMATIONAL PHASE BEHAVIOR OF SINGLE POLYMERS

As T decreases, polymers undergo a coil to globular transition. Such a collapse transition takes place in a continuous manner, therefore the heat capacity C_v of the polymer has a modest peak or a shoulder-like structure at the transition temperature T_θ [5, 6], because N is not large. We calculated C_v using fluctuation in the potential energy E ,

$$C_v = \frac{1}{k_B T^2} (\langle E^2 \rangle - \langle E \rangle^2). \quad (5)$$

Figure 2 (A) shows that C_v increases with a decrease in T with a shoulder at $T \simeq 2.3$ (the black dashed line). In Figure 2 (B), we plotted the radius gyration $R_g = \sqrt{\frac{1}{N} \sum_1^N (\vec{r}_i^2 - \vec{r}_{cm})^2}$ as a function of T , where \vec{r}_i and \vec{r}_{cm} are position vectors of the i -th monomer and the center of mass of the single polymer, respectively. Figure 2 (B) shows that the size of the single polymer changes rather sharply near $T = 2.3$, which confirms that the coil-to-globule transition occurs at $T_\theta = 2.3$.

When T goes below T_θ , the globular single polymers may become “crystalline” at the temperature $T_M < T_\theta$. In our single polymer model, however, the crystallization is suppressed in the range of T that we considered ($0.35 \leq T \leq 4.35$).

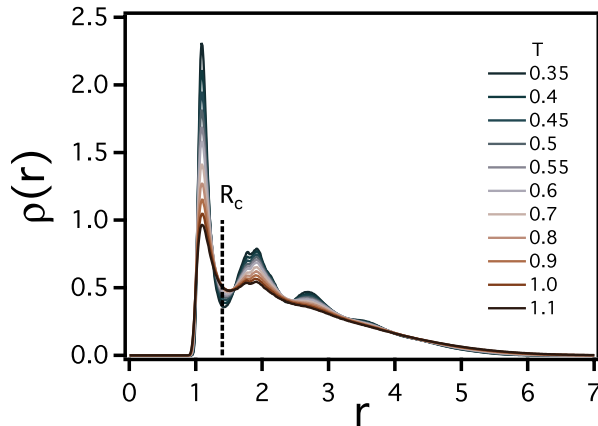


FIG. 3. The radial distribution function $\rho(r)$ of non-bonded monomers at various T . $\rho(r)$ is defined as $\rho(r) = \frac{1}{N_{non}} \sum_{(i,j)'} \delta(|r_i - r_j| - r)$, where N_{non} is the number of non-bonded pairs and $(i,j)'$ indicates that the sum is over all non-bonded pairs of monomers. The discretized peaks, a signature of the ordered spatial arrangement of monomers, are not observed in all range of T . $\rho(r)$ has the first minimum at near $R_c = 1.4$ (the black dashed line), which is used as a cut-off length when we define a contact between $q_{i,j}$ monomers i and j (see the main text).

The crystallization of the single polymer is a first-order conformational transition, such that E and R_g change abruptly at T_M where C_v has a sharp peak [5]. These interesting features are not observed in Figure 2. In addition, the radial distribution function $\rho(r)$ of the monomers in Figure 3 confirms again that the spatial arrangement of the monomers is still disordered even at the lowest T .

III. VERIFICATION OF THE METASTABLE STATES IN THERMODYNAMIC LIMIT

In the main text, we established that the first order transition in Q_{stat} occurs as $\epsilon (\neq 0)$ varies, proving the existence of the metastable states of the SCP when $N = 128$. However, this does not, in principal, guarantee that the metastable states of the SCP should appear in thermodynamic limit ($N \rightarrow \infty$), since we considered only one length of single polymers. In this section, by illustrating that apparent first order transition in Q_{stat} takes place at larger N , we confirm the existence of the metastable states for larger N as well. It is likely that the transitions become sharper for $N \gg 1$ although it is difficult to carry out these simulations using the FP method.

We carried out additional simulations for various N at $T = 0.9$ and determined ϵ_c . The distributions of Q_{stat} at ϵ_c ($P_{\epsilon_c}(Q_{stat})$) are depicted in Figure 4. When $N = 32$, $P_{\epsilon_c}(Q_{stat})$ has a single peak, indicating a likely continuous transition in the order parameter, Q_{stat} . As N increases to 256, the peak becomes broader and is split into two peaks.

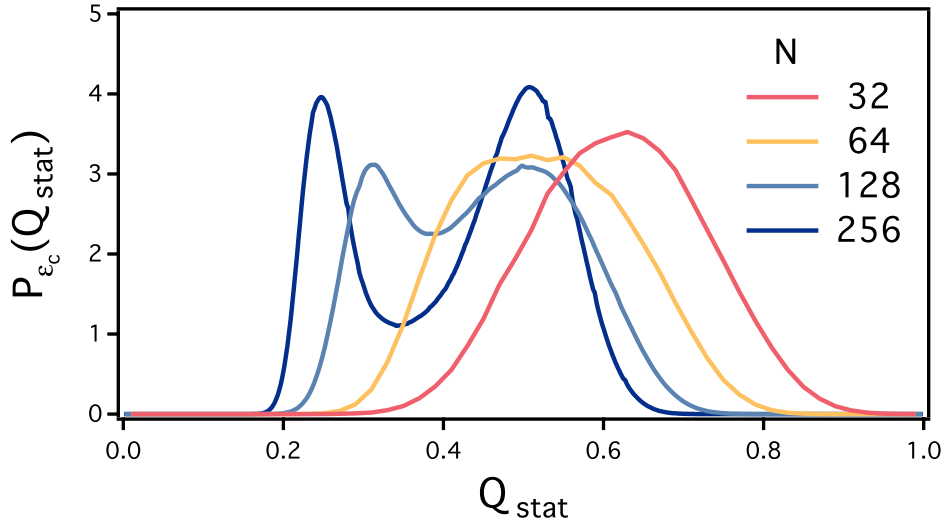


FIG. 4. $P_{\epsilon_c}(Q_{\text{stat}})$ at $T = 0.9$ for various N .

With an increase in N , the separation between the two peaks is more pronounced, and the concave character between them becomes deeper. Considering that the negative logarithm of $P_{\epsilon_c}(Q_{\text{stat}})$ is associated with the energy landscape of the transition (Eq (3) of the main text), this means that the metastable states in the SCP are separated by higher energy barriers as N increases, suggesting that the metastable states should exist more stably as $N \rightarrow \infty$.

IV. DETERMINATION OF T_d

According to the RFOT theory, the exponential number of metastable states emerge at or below the dynamic transition T_d [7], which for finite system would represent a rounded transition. Since in the FP method, the first-order transition characterized by Q_{stat} at non-zero ϵ_c is attributed to the existence of the metastable states, the first-order transition nature should disappear and the overlap order parameter should change continuously with ϵ when $T > T_d$ [8, 9]. Therefore, T_d of the single polymer can be determined as T where the first-order transition in Q_{stat} starts to vanish. In Figure 5, we show the distribution of the order parameters at the critical $\epsilon = \epsilon_c$, $P_{\epsilon_c}(Q_{\text{stat}})$, by varying T . For $T < 1.8$ (Figure 5 (A)), $P_{\epsilon_c}(Q_{\text{stat}})$ is bimodal, which is a signature of the first-order phase transition. On the other hand, when T exceeds 1.8 (Figure 5 (B)), $P_{\epsilon_c}(Q_{\text{stat}})$ becomes unimodal, implying that Q_{stat} changes continuously at $T \geq 1.8$. Hence, we determine that $T_d = 1.8$.

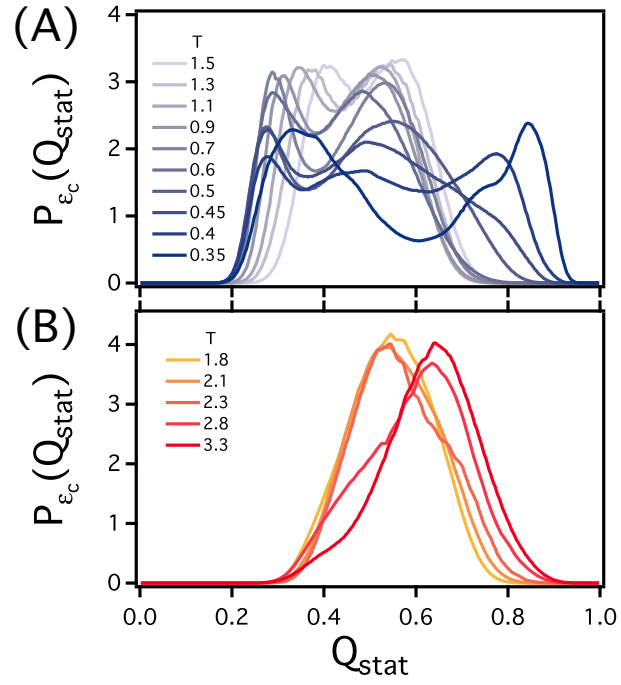


FIG. 5. $P_{\epsilon_c}(Q_{stat})$ for (A) $T < 1.8$ and (B) $T \leq 1.8$.

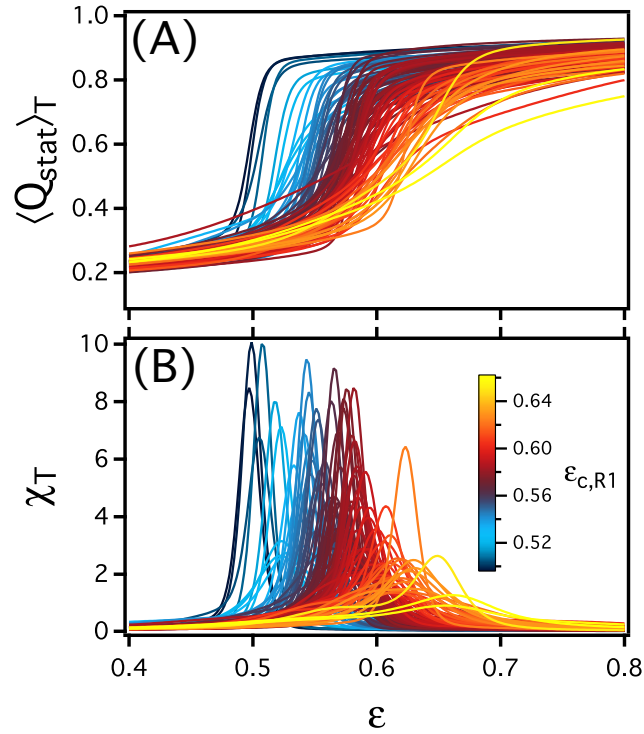


FIG. 6. (A) The average and (B) the susceptibility of Q_{stat} as a function of ϵ for given configurations $\{\vec{r}_0^i\}$ in Replica 1 at $T = 0.35$. Individual curves are colored according to their ϵ_c (the color bar in (B)), where ϵ_c is defined as a peak position of χ_T in the lower panel.

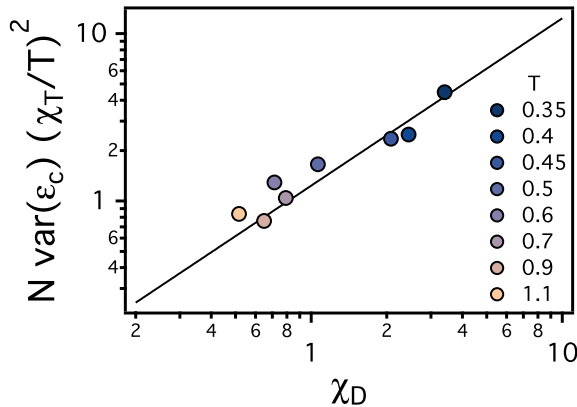


FIG. 7. Quantitative relation between χ_T and χ_D . The linear line ($y = 1.23x$) is obtained by curve fitting, which confirms the validity of Eq (7)

V. RANDOM FIELD ISING MODEL (RFIM) BEHAVIOR OF SINGLE POLYMERS

In the FP method for glassy liquids, the external coupling field (ϵ) introduces quenched disorder to the configuration $\{\vec{r}\}$ in Replica 2. The nature of the quenched disorder is determined by the reference configuration $\{\vec{r}_0\}$, which influences the critical fluctuations. Figure 6 illustrates the influence of the disorder on the critical behavior of the order parameters. In Figure 6 (A), we considered 112 $\{\vec{r}_0\}$ at $T = 0.35$ and the estimated the averages of $\langle Q_{\text{stat}} \rangle_T$ with respect to ϵ for individual $\{\vec{r}_0\}$, where $\langle \dots \rangle_T$ indicates the thermal average of the property for fixed ϵ and $\{\vec{r}_0\}$. We plot the corresponding susceptibilities χ_T in Figure 6 (B), where $\chi_T = N(\langle Q_{\text{stat}}^2 \rangle_T - \langle Q_{\text{stat}} \rangle_T^2)$. The figure shows that the transitions in Q_{stat} for various $\{\vec{r}_0\}$ take place at different values of ϵ with different extent of sharpness, corresponding to peak positions and heights of their χ_T . The contribution of the disorder to the critical behavior of Q_{stat} is quantified by decomposing the fluctuation χ_{stat} into the thermal (χ_T) and disorder (χ_D) contributions [9], where χ_D is defined as

$$\chi_D = N(\langle \langle Q_{\text{stat}}^2 \rangle_T \rangle_D - \langle \langle Q_{\text{stat}} \rangle_T \rangle_D^2), \quad (6)$$

and $\langle \dots \rangle_D$ denotes an average over $\{\vec{r}_0\}$ at a given T and ϵ . By definition, the sum of χ_D and χ_T is $\chi_{\text{stat}} = \chi_D + \chi_T$.

In glassy liquids, χ_D grows more rapidly than χ_T as T decreases. Quantitative relation between χ_D and χ_T is expressed as

$$\chi_D \simeq N \text{var}(\epsilon_c) \left(\frac{\chi_T}{T} \right)^2, \quad (7)$$

where $\text{var}(\epsilon_c)$ is the variance of the critical points among $\{\vec{r}_0\}$ [10–12]. In Figure 7, we plot $N \text{var}(\epsilon_c) \left(\frac{\chi_T}{T} \right)^2$ with

respect to χ_D for various T (the colored symbols), where ϵ_c of $\{\vec{r}_0\}$ is determined as a peak position of χ_T . The black solid line ($y \sim x$) confirms the validity of Eq (7), showing that χ_D and χ_T follows well Eq (7). This implies that as T approaches T_K , the disorder fluctuation of the single polymer makes the dominant contribution to the total fluctuations. This behavior is reminiscent of the phase transition behavior in the random field Ising model (RFIM) [13]. Therefore, we conclude that freezing in single polymeric glass when $\epsilon \neq 0$ could be in the same universality class as RFIM. The similarity between the RFIM-like behavior and that found in glass forming systems [10–12] further fortifies the conclusions reached in the main text that the low temperature properties of the SCP, and other compact polymers such as chromosomes, ought to exhibit glass-like behavior in the condensed state. We will be remiss if we did not add that at $T_K \sim T_c$ the transition has the character of the random first order transition at zero coupling strength.



- [1] D. Frenkel and B. Smit, *Understanding molecular simulation: from algorithms to applications.*, 2nd ed. (Academic Press, 1996).
- [2] L. Berthier, P. Charbonneau, D. Coslovich, A. Ninarello, M. Ozawa, and S. Yaida, “Configurational entropy measurements in extremely supercooled liquids that break the glass ceiling,” *Proc. Natl. Acad. Sci. USA* **114**, 11356–11361 (2017).
- [3] L. Berthier, “Overlap fluctuations in glass-forming liquids,” *Phys. Rev. E* **88**, 022313 (2013).
- [4] L. Berthier and D. Coslovich, “Novel approach to numerical measurements of the configurational entropy in supercooled liquids,” *Proc. Natl. Acad. Sci. USA* **111**, 11668–11672 (2014).
- [5] M. P. Taylor, W. Paul, and K. Binder, “Phase transitions of a single polymer chain: A wang-landau simulation study,” *J. Chem. Phys.* **131**, 114907 (2009).
- [6] D. F. Parsons and D. R. M. Williams, “An off-lattice wang-landau study of the coil-globule and melting transitions of a flexible homopolymer,” *The Journal of Chemical Physics* **124**, 221103 (2006).
- [7] T. R. Kirkpatrick, D. Thirumalai, and P. G. Wolynes, “Scaling concepts for the dynamics of viscous liquids near an ideal glassy state,” *Phys. Rev. A* **40**, 1045–1054 (1989).
- [8] S. Franz and G. Parisi, “Phase diagram of coupled glassy systems: a mean-field study,” *Phys. Rev. Lett.* **79**, 2486–2489 (1997).
- [9] L. Berthier and R. L. Jack, “Evidence for a disordered critical point in a glass-forming liquid,” *Phys. Rev. Lett.* **114**, 205701 (2015).
- [10] L. Berthier, G. Biroli, J.-P. Bouchaud, L. Cipelletti, D. El Masri, D. L’Hôte, F. Ladieu, and M. Pierno, “Direct experimental evidence of a growing length scale accompanying the glass transition,” *Science* **310**, 1797–1800 (2005).

- [11] L. Berthier, G. Biroli, J.-P. Bouchaud, W. Kob, K. Miyazaki, and D. R. Reichman, “Spontaneous and induced dynamic fluctuations in glass formers. i. general results and dependence on ensemble and dynamics,” *J. Chem. Phys.* **126**, 184503 (2007).
- [12] L. Berthier, G. Biroli, J.-P. Bouchaud, W. Kob, K. Miyazaki, and D. R. Reichman, “Spontaneous and induced dynamic correlations in glass formers. ii. model calculations and comparison to numerical simulations,” *The Journal of Chemical Physics* **126**, 184504 (2007).
- [13] D. S. Fisher, “Scaling and critical slowing down in random-field ising systems,” *Phys. Rev. Lett.* **56**, 416–419.